Supported by

U.S. DEPARTMENT OF ENERGY | Office of Science

Diagnostic options for radiative divertor feedback control on NSTX-Upgrade

Coll of Wm & Mary
Columbia U
CompX
General Atomics
FIU
INL
Johns Hopkins U
LANL
LLNL
Lodestar
MIT
Lehigh U
Nova Photonics
ORNL
PPPL
Princeton U
Purdue U
SNL
Think Tank, Inc.
UC Davis
UC Irvine
UCLA
UCSD
U Colorado
U Illinois
U Maryland
U Rochester
U Tennessee
U Tulsa
U Washington
U Wisconsin
X Science LLC

V. A. Soukhanovskii

S. P. Gerhardt, R. Kaita, A. G. McLean, R. Raman

and the NSTX Research Team

Culham Sci Ctr
York U
Chubu U
Fukui U
Hiroshima U
Hyogo U
Kyoto U
Kyushu U
Kyushu Tokai U
NIFS
Niigata U
U Tokyo
JAEA
Inst for Nucl Res, Kiev
Ioffe Inst
TRINITI
Chonbuk Natl U
NFRI
KAIST
POSTECH
Seoul Natl U
ASIPP
CIEMAT
FOM Inst DIFFER
ENEA, Frascati
CEA, Cadarache
IPP, Jülich
IPP, Garching
ASCR, Czech Rep

Poster P.6.18
19th Topical Conference High-Temperature Plasma Diagnostics
Monterey, CA, May 6-10, 2012

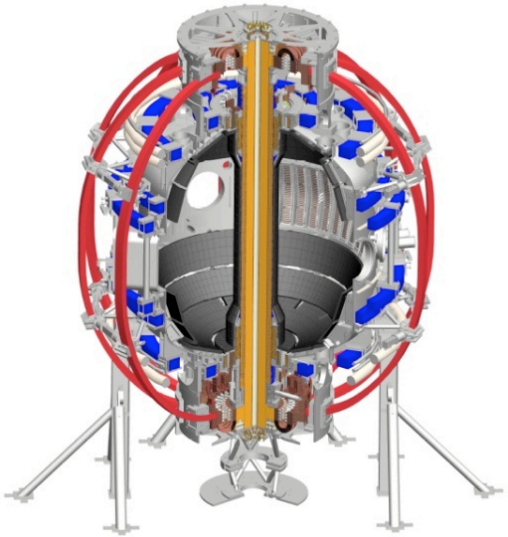

Outline - Developing real-time radiative divertor feedback control for NSTX-U

- Impurity-seeded radiative divertor technique is one of the leading candidates to mitigate divertor heat flux in NSTX-U discharges
  - Unmitigated 20-30 MW/m^2 peak heat fluxes predicted
- Radiative divertor feedback control being developed for NSTX-U
  - Proportional, integral, derivative process controller to be used in digital plasma control system
  - Fast piezoelectric valve is the actuator
    - Gas flow rate is proportional to control voltage
  - Control signal diagnostics for divertor detachment identification and control (System ID) are discussed in this poster
    - Divertor ID diagnostics
      - IR thermography
      - Thermoelectric current
      - Impurity VUV spectroscopy and bolometry
      - Neutral gas pressure
      - Electron-ion recombination rate via UV/NIR spectroscopy
    - Pedestal ID diagnostics

Abstract

A radiative divertor technique is used by present day tokamak experiments and planned for ITER to mitigate high heat loads on divertor plasma-facing components to prevent their excessive erosion and thermal damage. The radiative divertor uses induced plasma volumetric power and momentum losses to reduce heat and particle flux density on divertor target plates. Extrinsically seeded deuterium or impurity gases have been employed to control divertor parameters in several tokamak experiments via a real-time feedback control of the gas seeding rate, providing design guidelines for the radiative divertor control system in ITER [1].

In the National Spherical Torus Experiment (NSTX), a medium-size spherical tokamak with lithium-coated graphite plasma-facing components (PFC) and high divertor heat flux ($q_{peak} \leq 15$ MW/m^2, $q_{||} \leq 200$ MW/m^2 [2]), radiative divertor experiments employed deuterium, methane, and neon preprogrammed gas injections. A significant reduction of divertor peak heat flux simultaneously with good core H-mode confinement has been demonstrated [3]. In the NSTX-U device, steady-state peak divertor heat fluxes are projected to 20-30 MW/m^2 [2]. In this work we use NSTX radiative divertor results to analyze diagnostic options applicable to NSTX-U for real-time feedback control of divertor heat flux.

The divertor detachment process is device-specific w.r.t. seeding gas species, radiating impurity, and onset parameters, albeit universally measured signatures such as reduction of divertor q_{peak}, increase in divertor n_e and decrease in T_e to below 2-3 eV, increase in P_{rad}, reduction of particle flux density and increase in recombination rate. Characteristic detachment onset time and spatial extent define diagnostic requirements to the control signal: the time resolution 5-10 ms and the spatial resolution of 1 cm. Two-dimensional coverage might be desirable. Based on the NSTX divertor detachment signatures [3], we identify three categories of diagnostics that can be used for control signals: 1) PFC diagnostics (e.g., surface temperature, impurity influx measurements); 2) divertor plasma diagnostics (e.g., radiated power, impurity spectroscopy, neutral or impurity gas pressure, ion flux, divertor T_e and n_e, ion recombination measurements); 3) scrape-off layer and pedestal diagnostics (e.g., monitoring MARFEs or pedestal degradation signs). These radiative divertor signatures are analyzed for uniqueness and ranked in utility. Once the control signal is unambiguously linked to the radiative divertor state identification, it can be fed into a real-time plasma control system that uses an algorithm (e.g., the proportional-integral-derivative controller) to compare the control signal to the set value, quantify the difference, and feedback on the control signal using impurity seeding as an actuator.

[1] ITER Physics Expert Group on Divertor, Nucl. Fusion 39 (1999) 2391; Nucl. Fusion 47 (2007) 8203

[2] T. K. Gray et al., J. Nucl. Mater. 415 (2011) S360

[3] V. A. Soukhanovskii et al., Phys. Plasmas 16 (2009) 022501; Nucl. Fusion 49 (2009) 095025

Divertor heat flux mitigation is key for present and future fusion plasma devices

- **Radiative divertor** is envisioned for present and future devices (e.g. **ITER, ST-FNSF**) as the **steady-state** heat flux mitigation solution
  - Divertor q_{peak} < 10 MW/m^2
  - Large divertor radiated power fractions (f_{rad} = 0.50 - 0.80)
  - Integration with pedestal and core
  - Partial divertor strike point detachment is the most promising regime

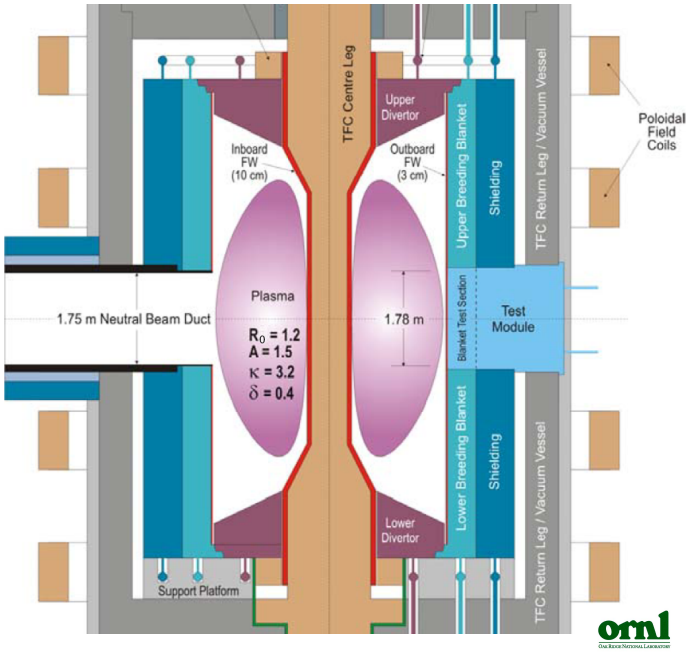

Peng et al, PPCF 47, B263 (2005)

$$q_{peak} \simeq \frac{P_{SOL}(1 - f_{rad}) f_{geo} \sin\alpha}{2\pi R_{SP} f_{exp} \lambda_{q_{\|}}}$$

$$A_{wet} = 2\pi R \, f_{exp} \, \lambda_{q_{\|}}$$

$$f_{exp} = \frac{(B_p/B_{tot})_{MP}}{(B_p/B_{tot})_{OSP}}$$

Multiple diagnostic measurements were needed to elucidate on radiative divertor physics in NSTX

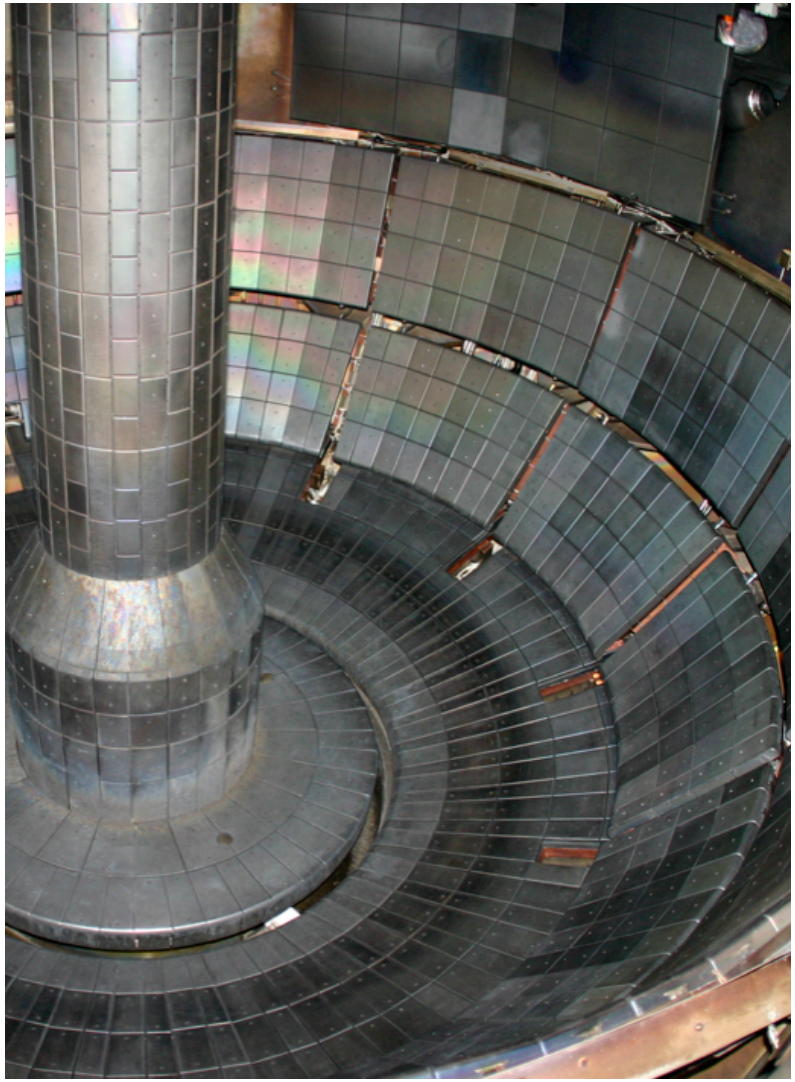

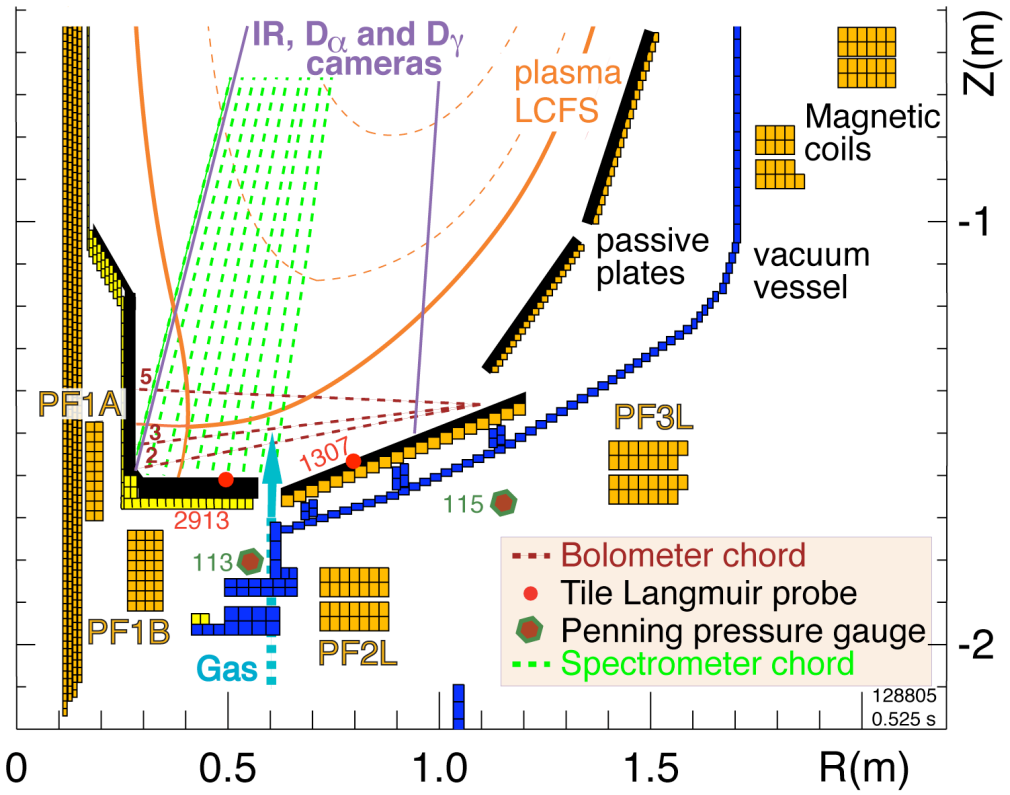

Plasma facing components

- ATJ and CFC tiles, lithium coatings
- Max P_{rad} fraction limited by impurity radiation efficiency (Li, C)
- Typical divertor tile temperature in 1 s pulses T < 500 C ($q_{peak} \leq 10$ MW/m^2)

Models used to simulate detachment operation space and divertor plasma parameters during detachment

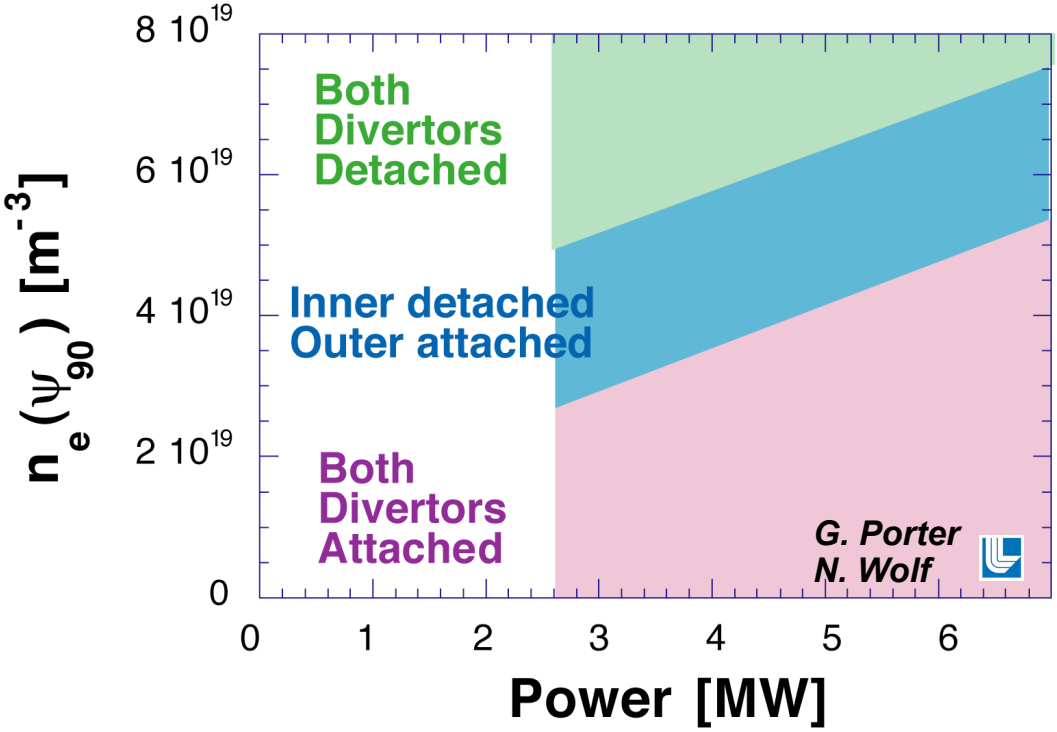

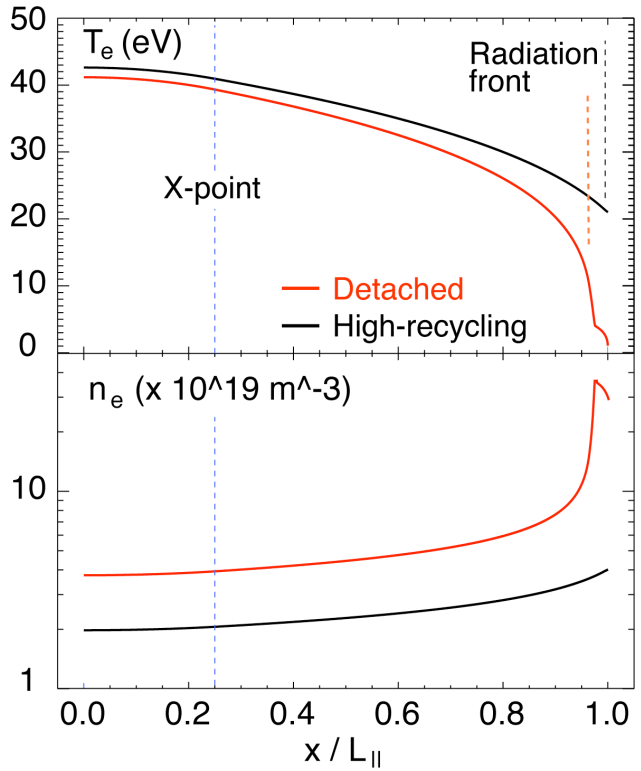

- Operating space P_{in}, n_e
- UEDGE calculations predicted limited "window" of outer divertor strike point detachment
- Radiation from intrinsic carbon at 3-5 %

- 5-zone 1D SOL model predicts typical T_e and n_e in NSTX during detachment
- High f_{rad} ~0.8-0.9 used for detachment simulation

SOUKHANOVSKII, V. et al., Phys. Plasmas 16 (2009) 022501,
SOUKHANOVSKII, V. et al., J. Nucl. Mater. 363-365 (2007) 432.

Radiative divertor experiments using low κ, δ configuration showed q_{peak} reduced albeit with confinement degradation

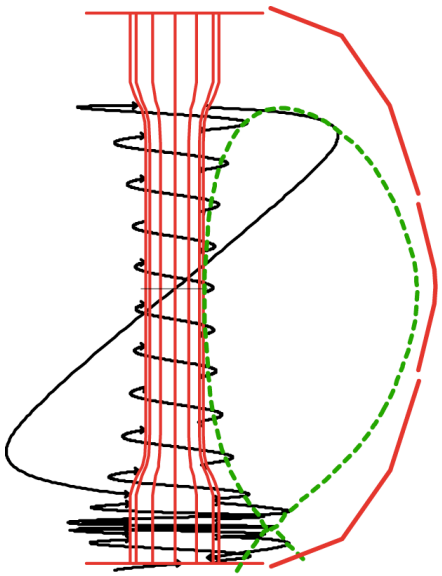

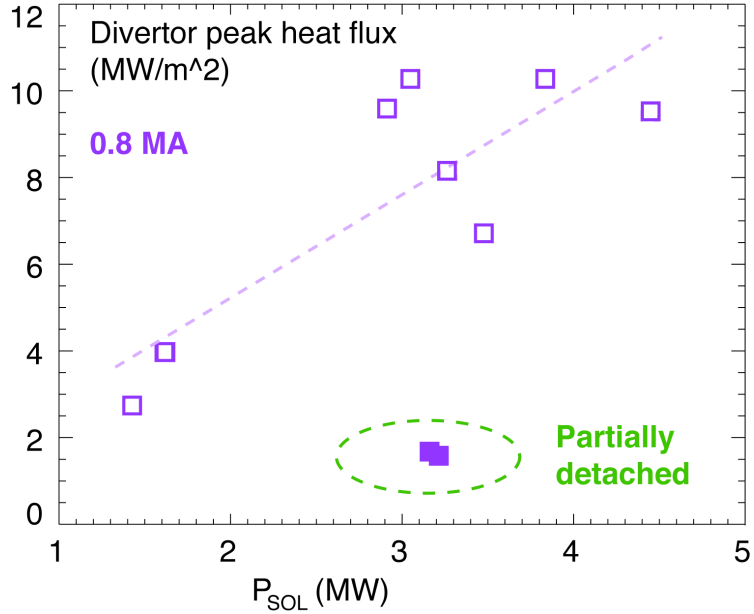

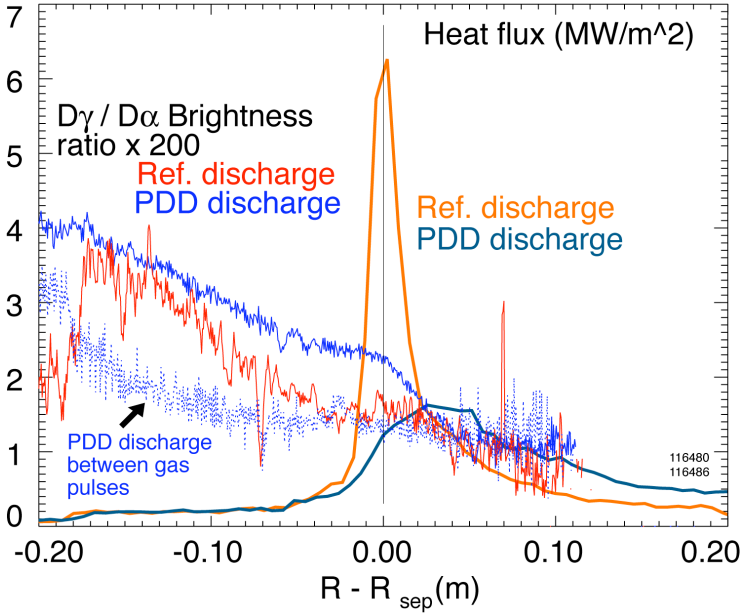

- Peak heat flux in outer divertor:
  - ITER-level q_{out}< 10-15 MW/m^2
  - Scaling of q_{peak}: linear with P_{sol} (P_{NBI}), linear-monotonic with I_p
  - Large q_{peak} asymmetry - 2-10; inner divertor always detached
- Experiments using D_2 injection:
  - q_{peak} reduced by up to 60 % in transient detachment regime
  - X-point MARFE degraded confinement within 2-3 x τ_E

GRAY, T. et al., J. Nucl. Mater. 415 (2011) S360,
SOUKHANOVSKII, V. et al., IAEA FEC 2006

Good core plasma performance and significant q_{peak} reduction obtained in high κ, δ detached divertor

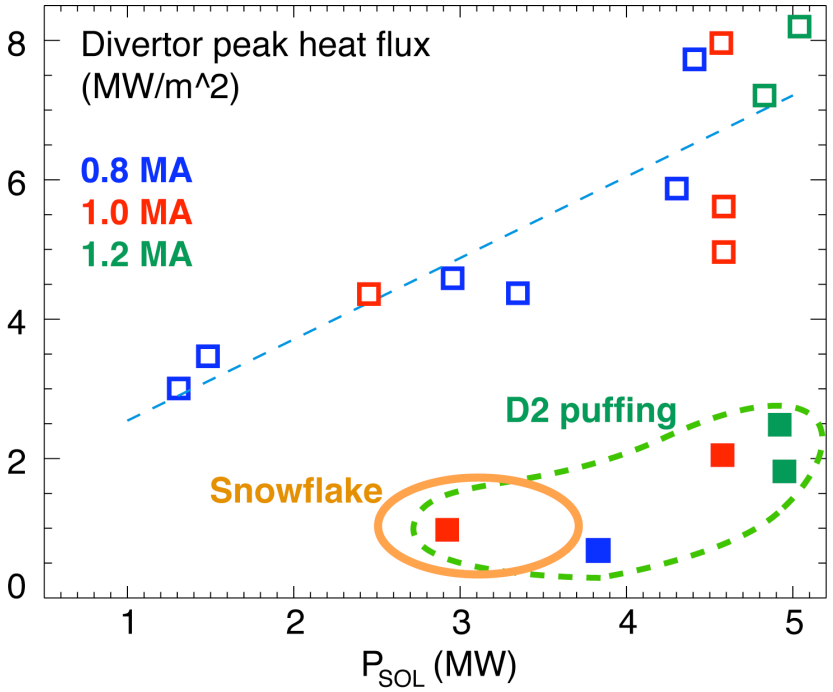

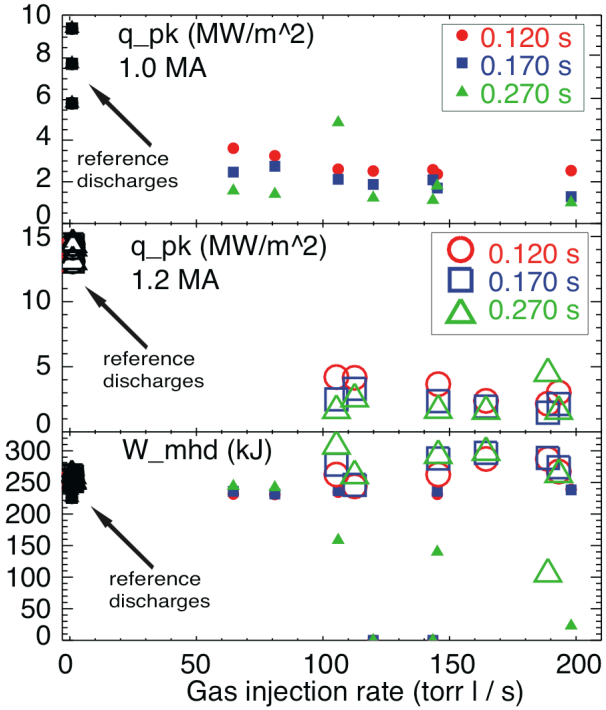

- Experiments conducted in 0.8-1.2 MA 4-6 MW NBI-heated H-mode discharges with κ=2.2-2.3, δ=0.6-0.75
- Obtained partially detached divertor outer strike point using divertor D_2 injection; P_{rad} due to intrinsic carbon
- q_{peak} reduced by 60 - 80 % with min. confinement degradation

SOUKHANOVSKII, V. et al., Phys. Plasmas 16 (2009) 022501,
SOUKHANOVSKII, V. et al., Nucl. Fusion 49 (2009) 095025

NSTX Upgrade will address critical plasma confinement and sustainment questions by exploiting 2 new capabilities

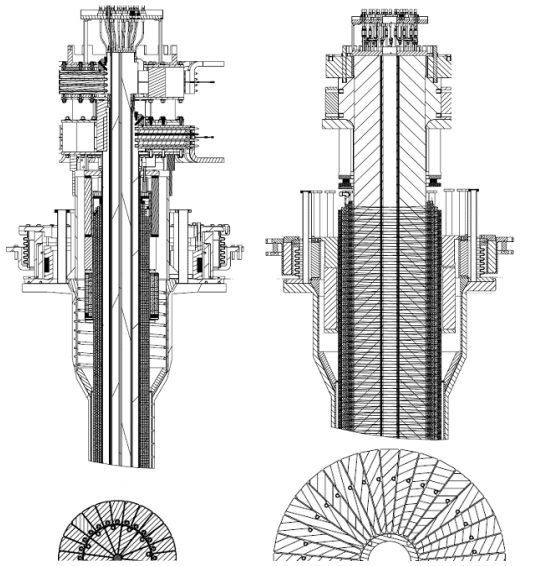

TF OD = 20cm
Previous
center-stack

TF OD = 40cm
New
center-stack

New center-stack

- **Reduces ν^* → ST-FNSF values to understand ST confinement**
  - Expect 2x higher T by doubling B_T, I_P, and NBI heating power
- **Provides 5x longer pulse-length**
  - q(r,t) profile equilibration
  - Tests of NBI + BS non-inductive ramp-up and sustainment

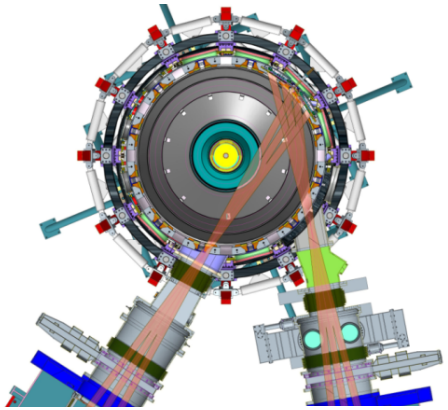

Present NBI

New 2nd NBI

New 2nd NBI

- **2x higher CD efficiency from larger tangency radius R_{TAN}**
- **100% non-inductive CD with q(r) profile controllable by:**
  - NBI tangency radius
  - Plasma density
  - Plasma position

MENARD, J. et al., Proceedings of the 24th IEEE Symposium on Fusion Engineering (2011).

NSTX-U scenarios with high I_p and P_{NBI} are projected to challenge passive cooling limits of graphite divertor PFCs

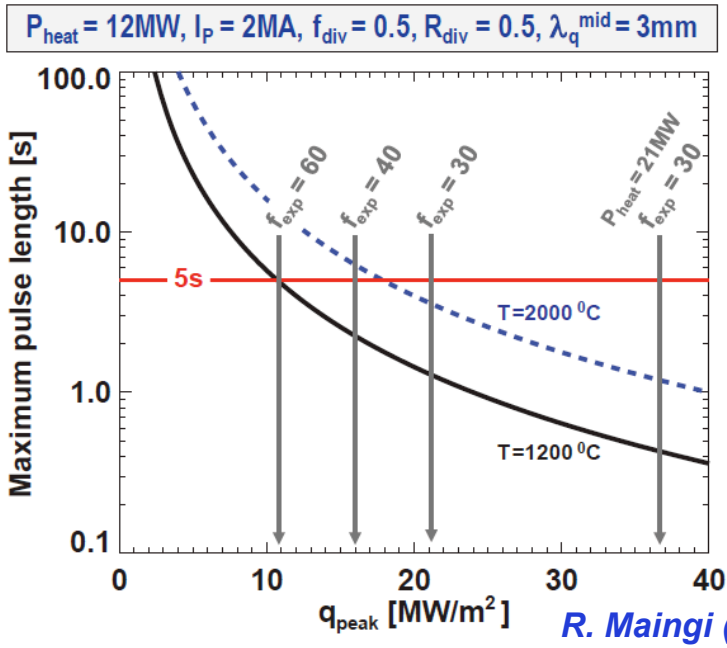

R. Maingi (ORNL)

NSTX Upgrade Scenarios

Device and scenario	NSTX-U 100% NICD		NSTX-U Long-pulse		NSTX-U Max I_P		NSTX-U Max I_P, P_{heat}		NSTX-U 100% NICD		NSTX-U Max I_P		NSTX-U High f_{BS}	
Confinement scaling	H98y2	H98y2	H98y2	H98y2	H98y2	H98y2	H98y2	H98y2	ST	ST	ST	ST	ST	ST
I_P [MA]	1.10	1.02	0.90	0.90	2.00	2.00	2.00	2.00	1.50	1.46	2.00	2.00	1.11	1.16
B_T [Tesla]	1.00	1.00	0.75	0.75	1.00	1.00	1.00	1.00	1.00	1.00	1.00	1.00	1.00	1.00
Aspect ratio A	1.7	1.7	1.7	1.7	1.7	1.7	1.7	1.7	1.7	1.7	1.7	1.7	1.7	1.7
R_0 [m]	0.93	0.93	0.93	0.93	0.93	0.93	0.93	0.93	0.93	0.93	0.93	0.93	0.93	0.93
Elongation κ	2.75	2.75	2.75	2.75	2.75	2.75	2.75	2.75	2.75	2.75	2.75	2.75	2.75	2.75
P_{NBI} [MW]	10.0	10.0	5.0	5.0	10.0	10.0	15.0	15.0	6.0	6.0	6.0	6.0	2.0	2.0
P_{RF} [MW]	0.0	0.0	0.0	0.0	0.0	0.0	4.0	4.0	0.0	0.0	0.0	0.0	2.0	2.0
P_{ind} [MW]	0.00	0.00	0.05	0.08	0.23	0.37	0.10	0.18	0.00	0.00	0.10	0.21	0.00	0.00
P_{heat} [MW]	10.0	10.0	5.05	5.08	10.2	10.4	19.1	19.2	6.00	6.00	6.10	6.21	4.00	4.00
Greenwald fraction	0.50	1.00	0.50	1.00	0.50	1.00	0.50	1.00	0.50	1.00	0.50	1.00	0.50	1.00
n_e-bar [10^{20}m^{-3}]	0.54	1.00	0.44	0.88	0.98	1.96	0.98	1.96	0.73	1.43	0.98	1.96	0.59	1.23
I_P flat-top time [s]	5.0	5.0	10.0	10.0	5.0	5.0	0.3	0.3	5.0	5.0	5.0	5.0	5.0	5.0
$\tau_{current\text{-}redistribution}$ [s]	1.04	0.57	0.65	0.37	1.37	0.79	1.83	1.05	2.41	1.13	2.23	1.05	1.76	0.81
# redistribution times	4.8	8.7	15	27	3.6	6.3	0.2	0.3	2.1	4.4	2.2	4.8	2.8	6.2
Stored energy [MJ]	0.68	0.54	0.36	0.33	0.96	1.08	1.35	1.37	1.04	1.00	1.20	1.26	0.65	0.70
β_N [%mT/MA]	5.4	4.6	4.7	4.2	4.2	4.7	5.9	5.9	6.0	6.0	5.2	5.5	4.9	5.0
β_T [%]	10.3	8.2	9.8	8.8	14.7	16.4	20.5	20.8	15.8	15.3	18.3	19.1	9.9	10.7
q*	6.8	7.3	6.2	6.2	3.7	3.7	3.7	3.7	5.0	5.1	3.7	3.7	6.2	5.9
Power fraction to divertor	0.50	0.50	0.50	0.50	0.50	0.50	0.50	0.50	0.50	0.50	0.50	0.50	0.50	0.50
$R_{strike\text{-}point}$ [m]	0.50	0.50	0.50	0.50	0.50	0.50	0.50	0.50	0.50	0.50	0.50	0.50	0.50	0.50
SOL heat-flux width [mm]	7.9	8.9	10.9	10.9	3.0	3.0	3.0	3.0	4.8	5.0	3.0	3.0	7.8	7.3
Poloidal flux expansion	22	22	22	22	62	62	62	62	22	22	38	38	22	22
Peak heat flux [MW/m^2]	9.1	8.1	3.4	3.4	8.7	8.8	16.2	16.2	9.0	8.6	8.4	8.6	3.7	4.0
Time to T_{PFC} = 1200°C [s]	6.1	7.6	44	44	6.7	6.5	1.9	1.9	6.1	6.7	7.1	6.8	36	31
Fraction of T_{PFC} limit	0.96	0.76	0.24	0.24	0.97	1.00	0.94	0.95	1.00	0.91	0.92	0.96	0.16	0.19

- High I_P scenarios projected to have narrow λ_q^{mid} → ~3mm
  - At high power, peak heat flux ≥ 9MW/m^2 even with high flux expansion ~60 with U/L snowflake
  - Numbers shown ignore radiation, plate tilt, strike-point sweeping

- **Passive cooling ok for low-I_P scenarios**
- **Long-pulse + high I_P and power may ultimately require active divertor cooling**

MENARD, J. et al., Proceedings of the 24th IEEE Symposium on Fusion Engineering (2011).

Radiative divertor control options are affected by NSTX-U plasma-facing component development plan

- Developing PFC plan to transition to full metal coverage for FNSF-relevant PMI development
- Wall conditioning: GDC, lithium and / or boron coatings
- PFC bake-out at 300-350°C

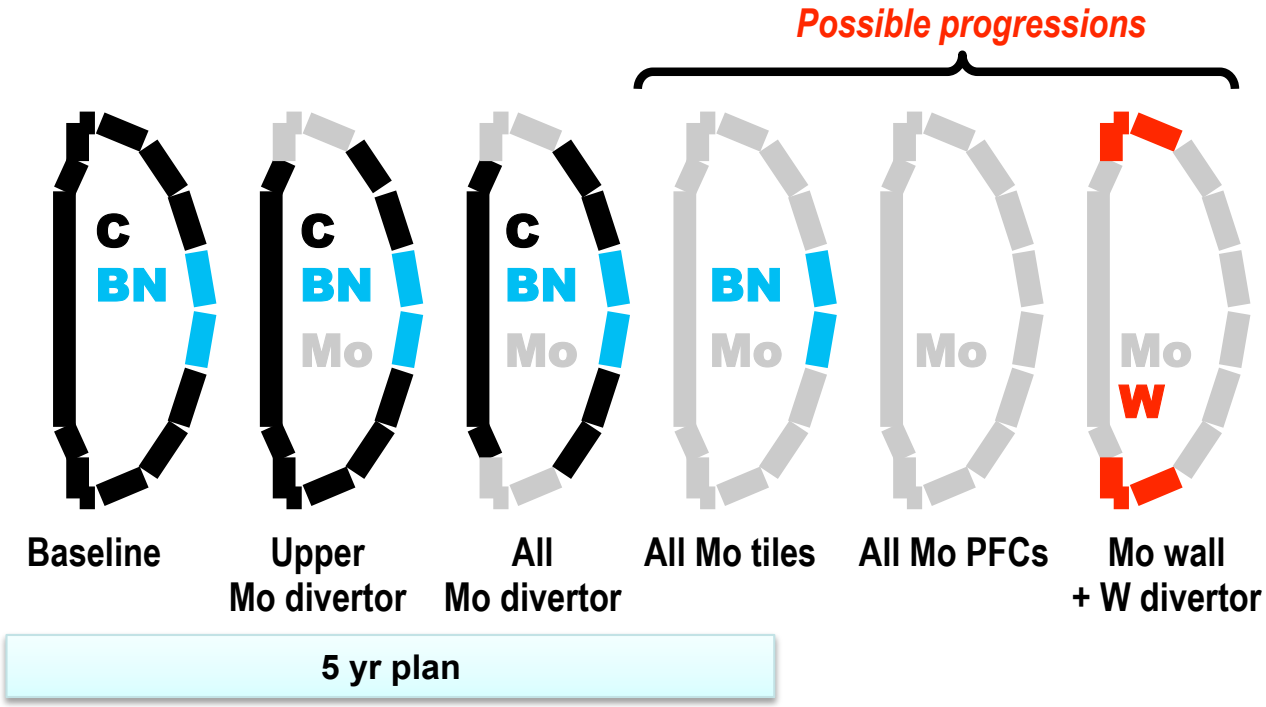

- Radiative divertor elements affected by PFC choice:
  - Divertor impurity gas handling and injection system
    - D_2, CD_4, Ar with graphite PFCs and lithium coatings
    - D_2, N_2, CD_4, Ar with refractory metal PFCs
  - Diagnostic sensors for control
  - Plasma Control System development

Mo tiles

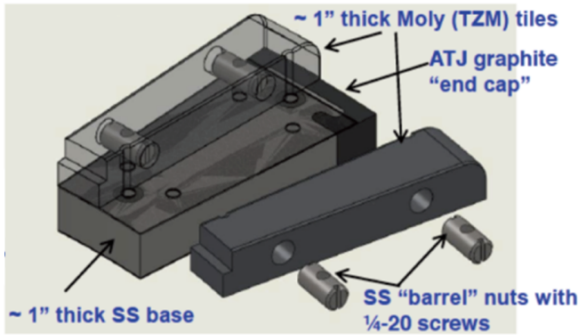

Impurity-seeded radiative divertor with feedback and snowflake geometry are the leading NSTX-U heat flux mitigation candidates

- NSTX-U scenarios with high I_p and P_{in} projected to challenge thermal limits of graphite divertor PFCs
- Single and double-null radiative divertors and upper-lower snowflake configurations considered
  - Supported by NSTX-U divertor coils and compatible with coil current limits
- Snowflake divertor projections to NSTX-U optimistic
  - UEDGE modeling shows radiative detachment of all snowflake cases with 3% carbon and up to P_{SOL}~11 MW
    - q_{peak} reduced from ~15 MW/m^2 (standard) to 0.5-3 MW/m^2 (snowflake)
- Snowflake divertor with impurity seeding for P_{SOL} ~ 20 MW under study

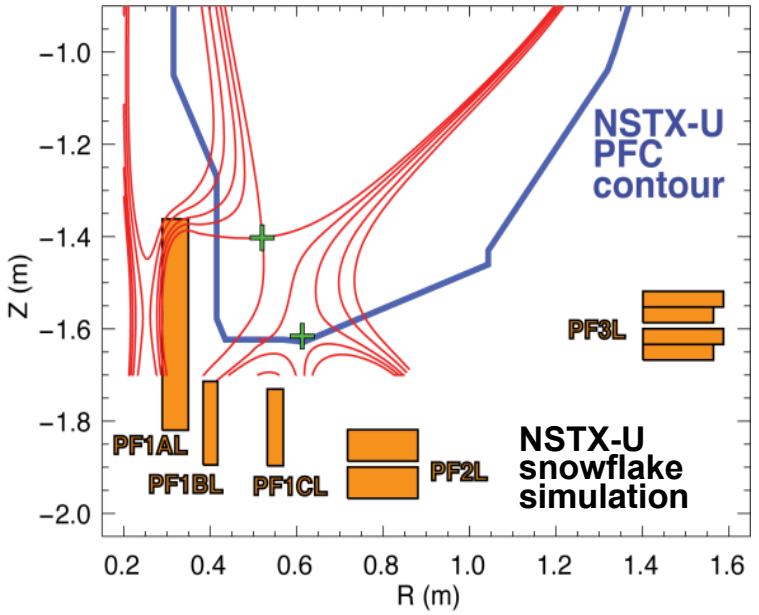

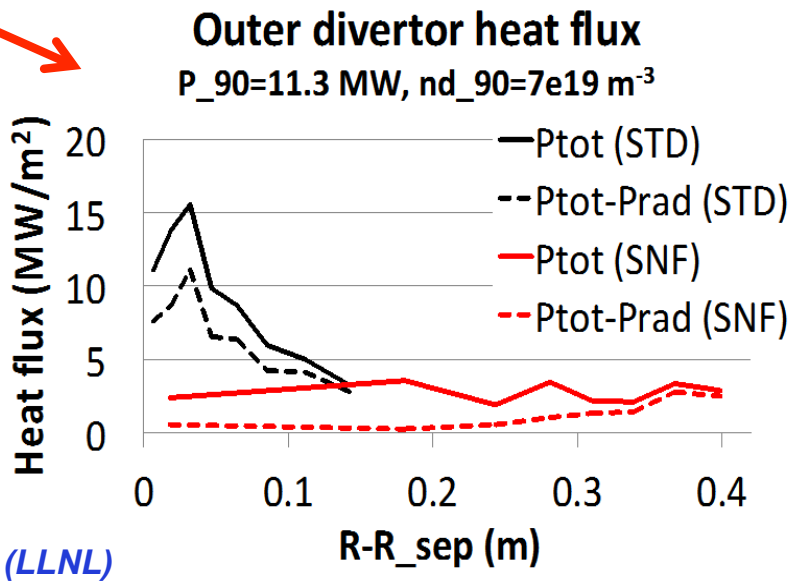

E. Meier (LLNL)

Conceptual design of radiative divertor feedback control system is based on PID control

- Proportional, integral, derivative controller

$$\Delta S = S_c - S_{ref}$$

$$V = K_0 + K_p \Delta S + K_i \int_{t_1}^{t_2} \Delta S dt + K_d \frac{d\Delta S}{dt}$$

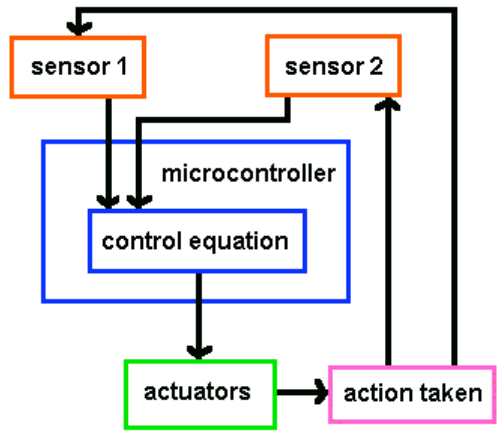

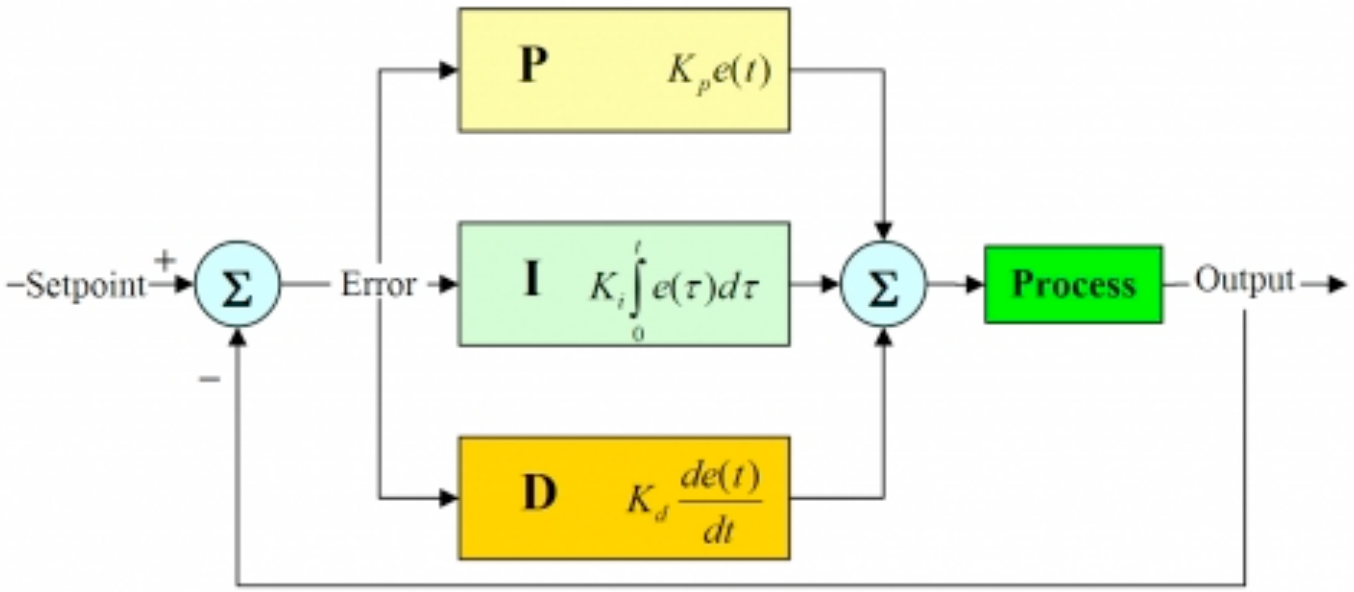

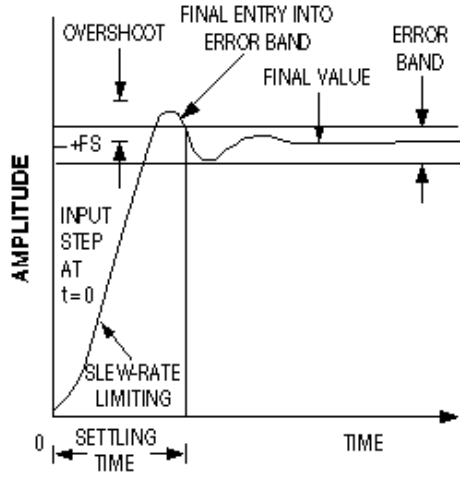

Control signal options demonstrated using divertor outer strike point partial detachment with D_2 or CD_4 puffing

- 4MW NBI-heated H-mode
  - CD_4 injection preprogrammed wave form
- Outer strike point detachment occurred at about 0.7 s (red traces)
  - Characteristic onset time 50 ms
- Divertor detachment affected divertor power balance
  - Carbon radiation and P_{rad} increased
  - Divertor heat flux decreased
- Divertor detachment affected SOL momentum balance
  - Neutral pressure increased (also due to gas puffing)
  - Divertor volumetric recombination rate increased (Balmer line intensities increased)

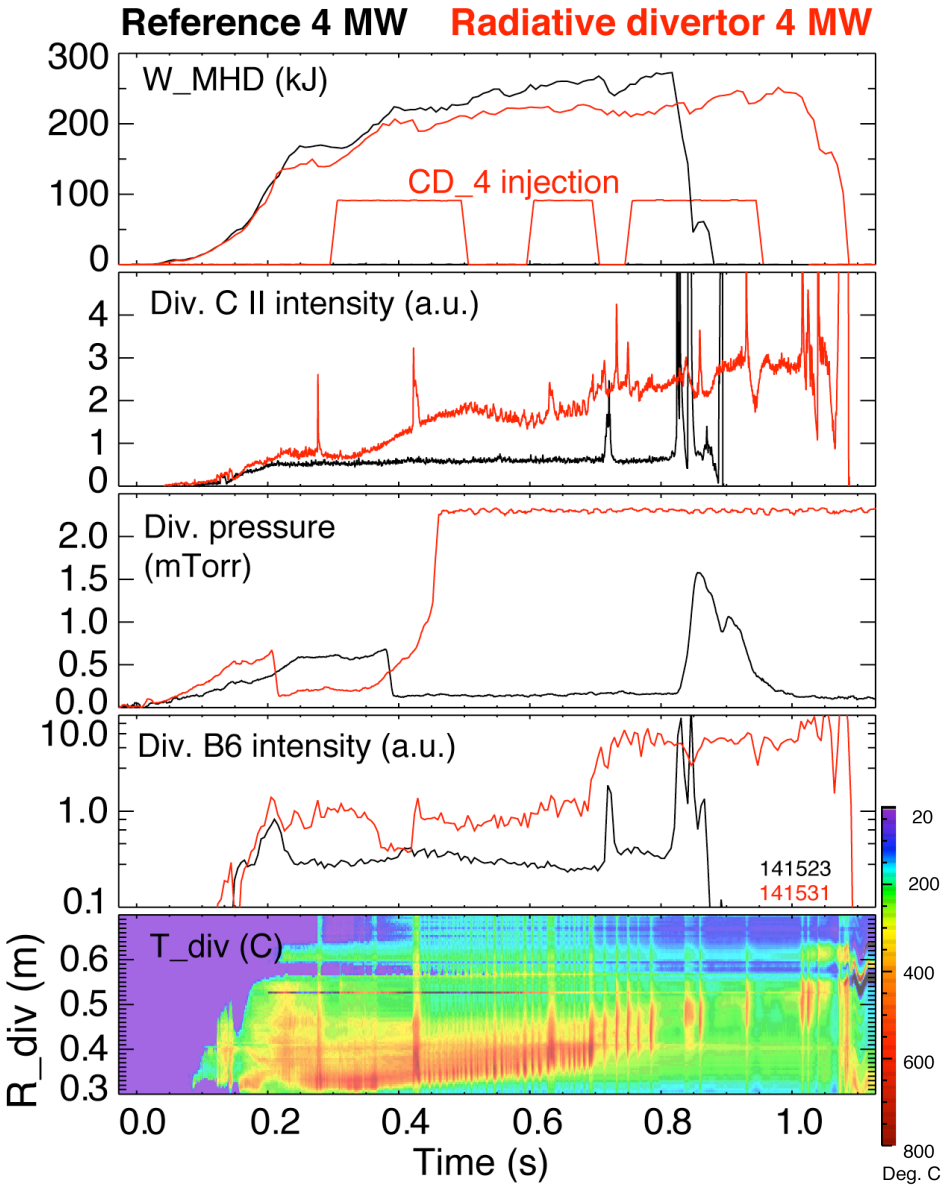

Option 1: IR thermography for divertor surface temperature monitoring

- Diagnostic principle and description
  - Measure PFC surface IR emission, calibrate for temperature
  - IR arrays (1D or 2D) or single-channel IR diode with strike-point region view
- Signal details from NSTX experiments
  - Detached region localization: 5-12 cm
  - Characteristic time: 1 ms
  - X 4 reduction during detachment
- Advantages:
  - Direct PFC temperature monitoring
- Issues:
  - Toroidal and poloidal localization
  - Interpretation and calibration issues due to PFC coatings (e.g., lithium)
- Implementation
  - Needs special IR and relay optics
  - IR optics

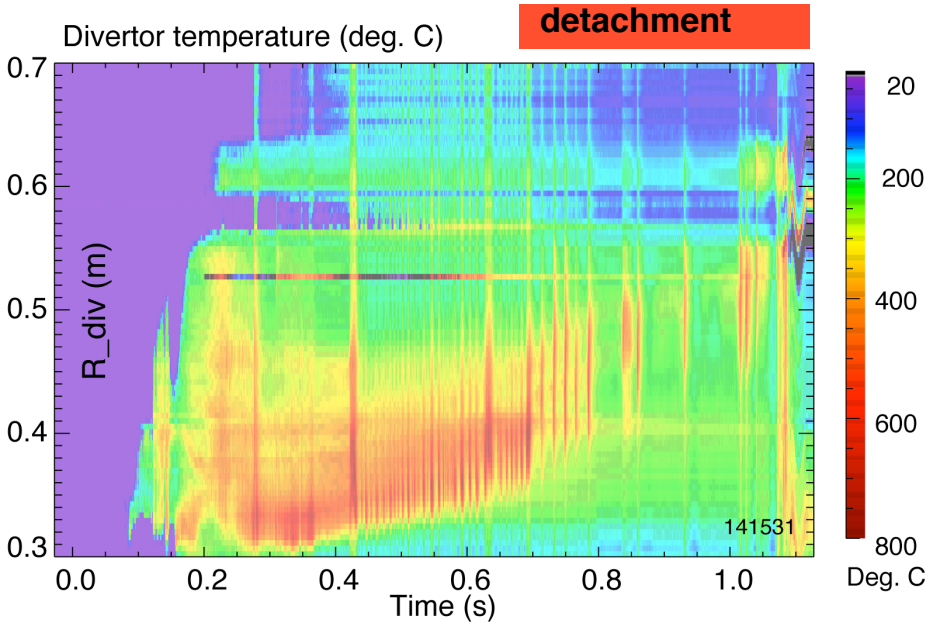

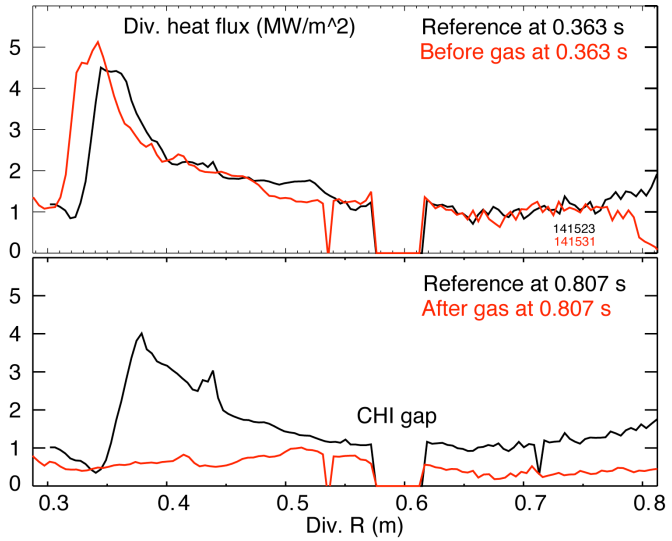

AHN, J.-W. et al., Rev. Sci. Instrum. 81 (2010) 023501.

Option 2: monitor SOL thermo-electric current representative of divertor electron temperature

- Diagnostic principle and description
  - SOL thermoelectric current due to divertor T_e difference
  - Electric current and potential
- Signal details from NSTX experiments
  - In NSTX inner and outer vessels electrically isolated
  - Potential V measured in CHI exp's

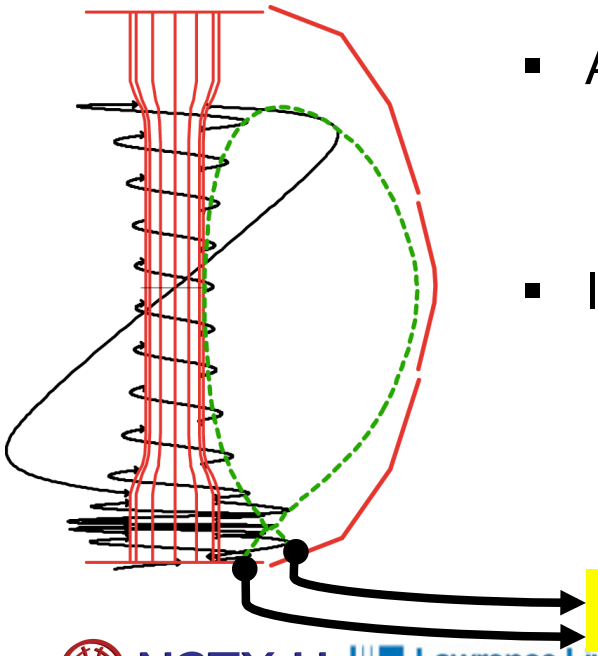

- Advantage:
  - Toroidally-averaged current and potential, linked to divertor T_e
- Issues:
  - More experiments needed to improve interpretation

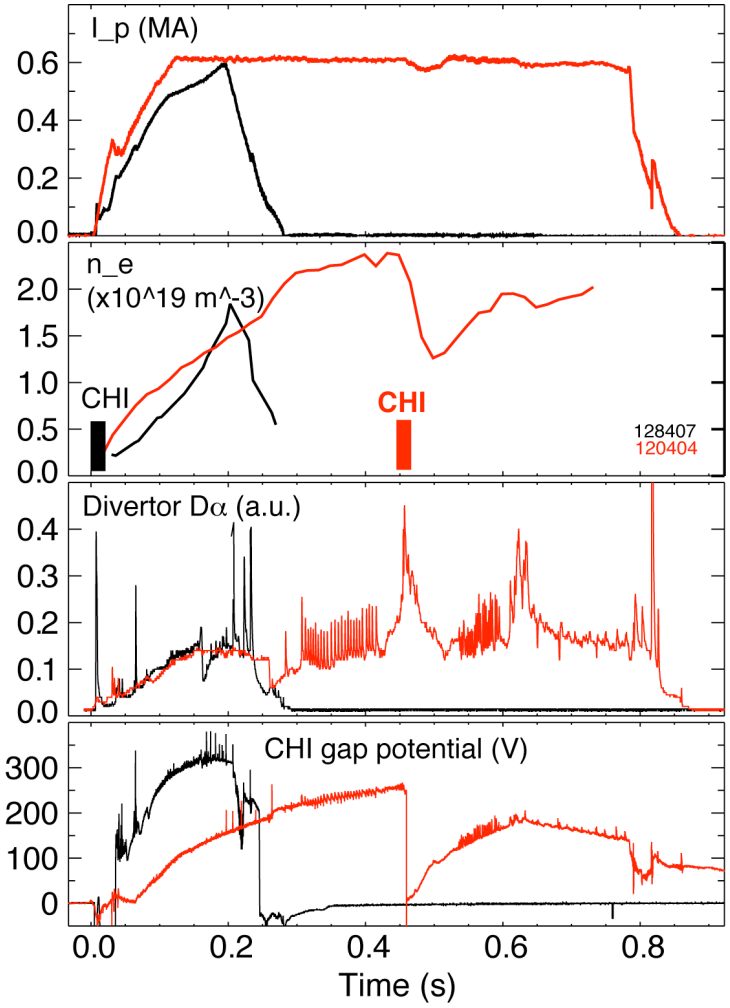

RAMAN, R. et al., Nucl. Fusion 49 (2009) 065006
STAEBLER, G. et al., Nucl. Fusion 29 (1989) 1820
KALLENBACH, A. et al., J. Nucl. Mater. 290-293 (2001) 639

Option 3: Monitor divertor radiated power or spectroscopic representation of radiated power

- Diagnostic principle and description
  - Fast bolometer or AXUV diode (or array) to monitor divertor rad. power
  - VUV spectroscopy
- Advantage:
  - Toroidally-averaged quantity linked to seeded impurity radiation
- Issues:
  - Need to know radiation distribution and spectral composition
- Implementation
  - Existing AXUV diode array (s)
  - Divertor SPRED
  - Dedicated divertor VUV monitor

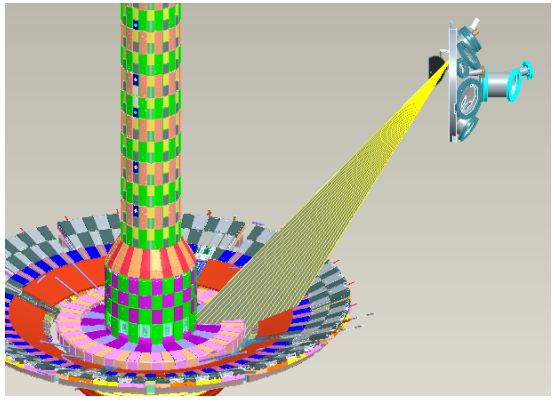

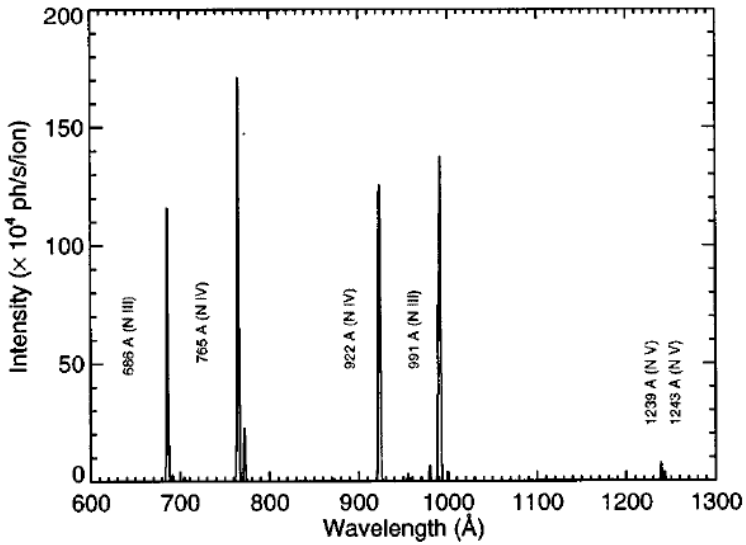

FIG. 2. Modeled N III, N IV, and N V spectrum at $T_e = 9.7$ eV and $n_e = 5 \times 10^{14}$ cm^{-3}. Calculated intensities were given a Gaussian profile with $\Delta\lambda_{FWHM} = 1$ Å.

SOUKHANOVSKII, V. et al., Rev. Sci. Instrum. 70 (1999) 340
SOUKHANOVSKII, V. et al., Rev. Sci. Instrum. 72 (2001) 3270

Option 4: Monitor neutral pressure

- Diagnostic description
  - Penning gauge for gas pressure monitoring in range 0.1-5 mTorr
- Signal details from NSTX experiments
  - Divertor pressure measured in private flux region, outer strike point region
- Advantages:
  - Direct seeding gas pressure measurement
- Issues:
  - Need to understand links to detachment characteristics
- Implementation
  - Straightforward, existing gauges can be used
  - Developing calibrated spectroscopic monitoring of Penning gauge

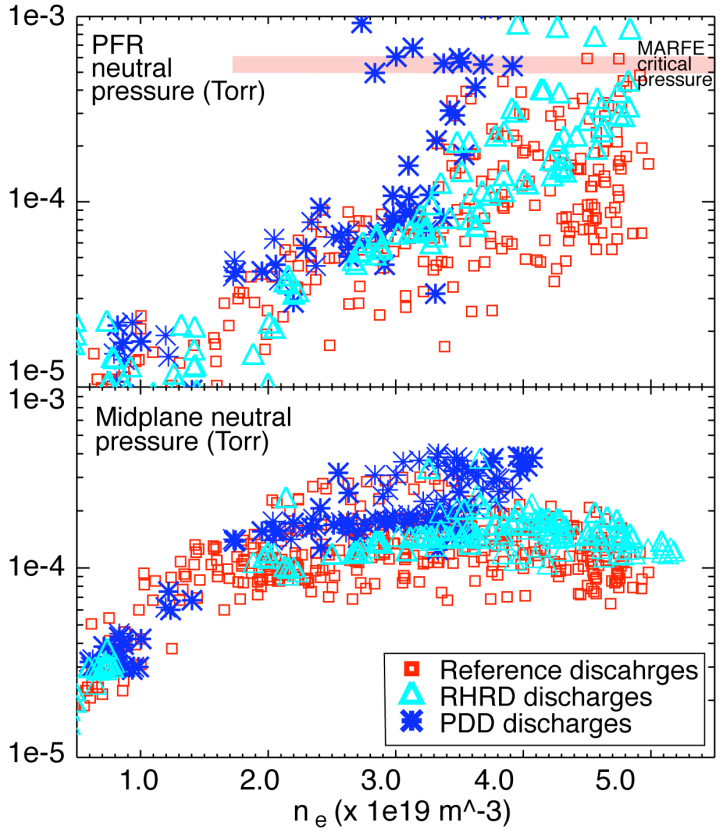

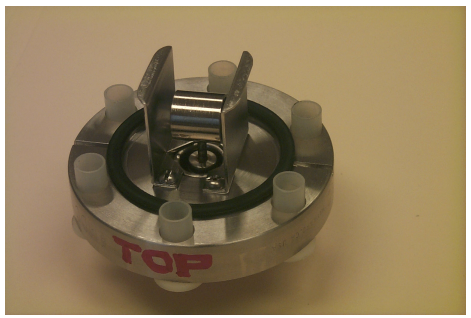

FINKEN, K. et al., Rev. Sci. Instrum. 63 (1992)

Option 5: Monitor recombination rate via Balmer or Paschen line spectroscopy

- Diagnostic description
  - UV or NIR spectroscopy to monitor emission line intensity from high-n Balmer or Paschen series lines
- Signal details from NSTX expt's
  - Strong indication of detachment, signal increases by up to 10^2
  - Observed *n*=2-*m*, m=3-12 (Balmer)
  - Observed *n*=3-*m*, m=5-10 (Paschen)
- Advantages:
  - Toroidally-averaged quantity
  - Direct measure of recombination rate
- Implementation
  - Can use existing UV and NIR fibers and instruments

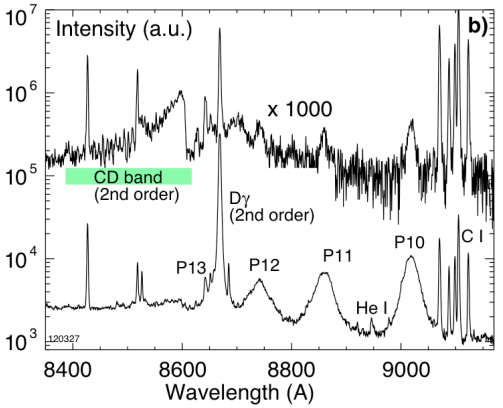

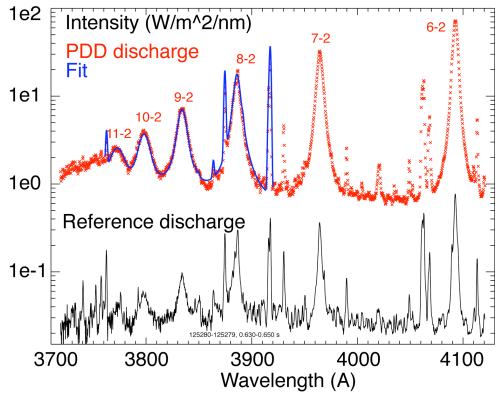

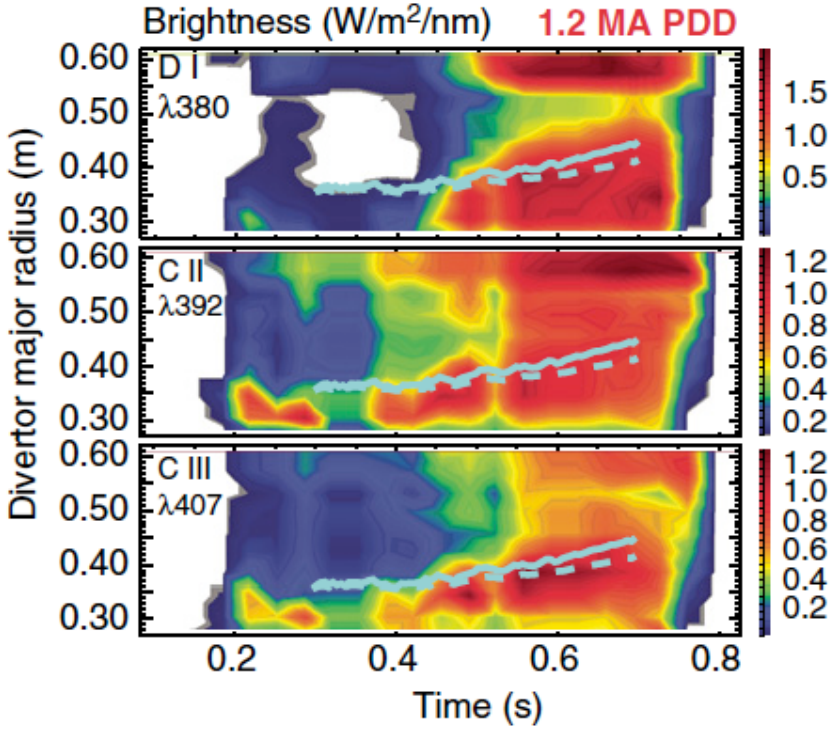

SOUKHANOVSKII, V. et al., Rev. Sci. Instrum. 77 (2006) 10127
SOUKHANOVSKII, V., Rev. Sci. Instrum. 79 (2008) 10539
SOUKHANOVSKII, V. et al., Rev. Sci. Instrum. 81 (2010) 10723.

Option 6: need "security" monitoring for signs of confinement degradation (pedestal temperature or MARFEs)

- Diagnostic principle and description
  - Monitor pedestal T_e (100-600 eV)
    - Soft X-ray arrays, real-time Thomson
  - Monitor MARFE formation
    - Edge neutral pressure
    - Divertor recombination rate

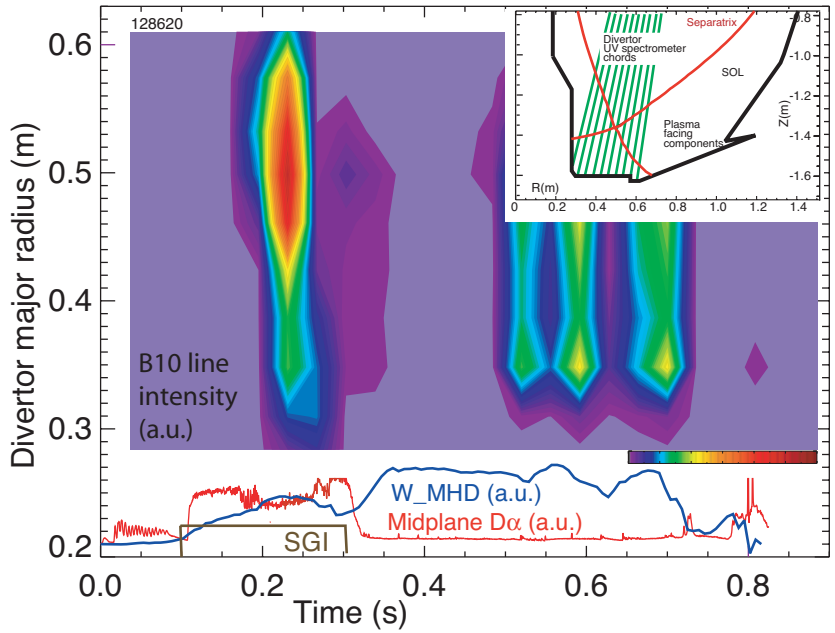

X-point MARFE formation during high-rate supersonic gas injection. Balmer B10 line intensity is plotted.

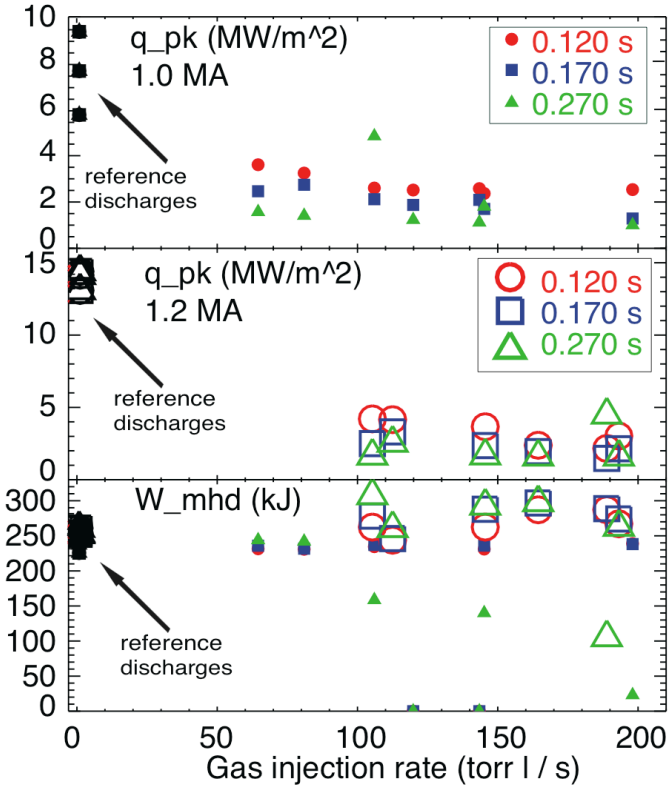

Optimal D_2 injection rate found (used 300 ms pulses)

- 50-100 Torr l /s for 1.0 MA discharges
- 110-160 Torr l /s for 1.2 MA discharges